

Evolution of atomic and electronic structure of Pt clusters: Planar, layered, pyramidal, cage, cubic, and octahedral growth

Vijay Kumar^{1,2} and Yoshiyuki Kawazoe²

¹*Dr. Vijay Kumar Foundation, 1969 Sector 4, Gurgaon, 122001 Haryana, India*

²*Institute for Materials Research (IMR), Tohoku University, Aoba-ku, Sendai 980-8577, Japan*

(Received 19 March 2008; published 13 May 2008)

Ab initio calculations on Pt clusters having diameters of up to about 3 nm show planar, layered, pyramidal, cage, simple cubic, and octahedral growth. Planar structures are preferred up to Pt₉, while layered and pyramidal structures are favored in the range of Pt_{*n*}, where $n=10-20$. In some cases, simple cubic and octahedral isomers become competitive with layered growth, or they have the lowest energy. Between $n=21$ and 24, decahedral isomers are most favorable with a decahedral (empty center) cage for Pt₂₂. Around $n=24$, there is again a transition and simple cubic structures become most favorable up to around $n=38$. Beyond this size, our results suggest octahedral isomers to be most favorable among the different growth modes explored by us, such as simple cubic, cuboctahedral, decahedral, and icosahedral. To our knowledge, platinum clusters are the first example of transition metal clusters that grow in bulk structure from a relatively small size range of $n\sim 40$ and for which a transition to commonly found closed packed icosahedral growth is unlikely. We find that a triangular isomer of Pt₆ and a square planar isomer of Pt₉ play the key role in the growth behavior and the formation of magic clusters of Pt that are rich in such triangular and/or square faces. Our results show that clusters with $n=6, 9, 10, 14, 18, 22, 27,$ and 36 with complete atomic shells are magic and are relatively more stable. In most cases, the clusters are weakly ferromagnetic. However, in some cases, a mixed ferromagnetic-antiferromagnetic coupling is obtained, such as that for Pt₆. The magnetic moments decrease with an oscillatory behavior as the size increases. The electronic structure of large octahedral clusters with $n\sim 200$ having (111) type faces develops similarity to bulk Pt (111) surface, but significant deviations exist that could lead to their different and size dependent behavior for reactions.

DOI: [10.1103/PhysRevB.77.205418](https://doi.org/10.1103/PhysRevB.77.205418)

PACS number(s): 73.22.-f, 36.40.Cg, 61.46.Bc, 82.20.Wt

I. INTRODUCTION

Platinum clusters and nanoparticles are industrially very important catalyst, such as in chemical reactions for clean environment, and play a vital role in fuel cells to produce hydrogen energy, which is attracting worldwide attention as a future source of clean energy. Great efforts are being made to improve efficiency and reduce the cost of such green technologies as well as to find cheaper alternatives to Pt due to escalation of its price. This has created wide interest in understanding the properties of Pt clusters and nanoparticles. Recently, magnetic moments have been reported¹ in small Pt clusters, although in bulk Pt is nonmagnetic. This is similar to the case of isoelectronic Pd, whose clusters are also magnetic.² However, the growth behaviors in the two cases are very different. Pd clusters favor an icosahedral (*I*) growth,² although recently for Pd₁₃, other structures have been found³ to be slightly lower in energy. However, Pt clusters, as we show here, favor relatively open structures, such as planar, layered, pyramidal, cage, simple cubic, and octahedral (*O*) growths. This makes clusters and nanoparticles of these two isoelectronic metals very distinct from each other and this could be one of the factors for their different catalytic properties. Also, clusters of Ni, which is in the same column in the Periodic Table as Pt, have icosahedral growth.⁴ Therefore, these results suggest a change in the growth behavior to less compact structures as one goes down in this column from Ni to Pt. Our results suggest that Pt clusters favor bulk structure at an early stage of growth and it is continued up to a fairly large size of ~ 3 nm diameter ex-

plored by us and that an *I* growth is unlikely. This could make Pt clusters unique among the transition metals.

Theoretical studies on Pt_{*n*} clusters by using *ab initio* methods are few beyond a size of $n\sim 10$. Clusters in the range of $n=2-20$ were reported⁵ to have relatively open structures, but an *I* structure was obtained for Pt₅₅. However, Apra *et al.*⁶ showed, using Pt₅₅ as an example, that Pt clusters have a tendency to amorphize. For Pt₁₃, there are a few studies. A cuboctahedron (*C*) was found⁷ to be lower in energy than an *I* isomer, but later, a low symmetry disordered structure was reported⁸ to be lower in energy than both the *I* and *C* structures. A buckled biplanar layered structure was also reported⁹ to be lower in energy than an *I* isomer. More recently, Futshek *et al.*¹⁰ studied small clusters of Pt having up to 13 atoms and found octahedral based structures in the range of 11–13 atoms. Wang and Johnson³ also did a detailed study of the 13-atom cluster by using *ab initio* molecular dynamics method and obtained lower energy isomers than known before. Their results showed a double layer triangular structure as well as a nine-atom planar structure with four-atom capping to be nearly degenerate for Pt₁₃ and lowest in energy. Larger clusters and nanoparticles of Pt are very important for applications but remain mostly unexplored. Clusters of many elements often have *I* growth, and in some cases, even if small clusters do not favor *I* growth such as for Au, i.e., an element adjacent to Pt in the Periodic Table, *I* growth becomes favorable as the size grows. However, our studies on a wide range of sizes of Pt clusters show that an *I* growth is not favorable at least up to a size of a few hundred atoms. Instead, we find planar, layered, pyramidal, cage, and

simple cubic structures to be among the lowest energy isomers in the small and intermediate size ranges of up to about 40 atoms, while O clusters are found to have the lowest energy for larger sizes. In Sec. II, we present the computational details of our calculations, while the results are given in Sec. III. A summary and discussion of the results is given in Sec. IV.

II. COMPUTATIONAL METHOD

The calculations have been performed by using *ab initio* ultrasoft pseudopotential (USP) and projected augmented wave (PAW) methods.^{11–14} Spin-polarized generalized gradient approximation¹⁵ has been used for the exchange-correlation energy. The clusters are placed in a large simple cubic unit cell with periodic boundary conditions so that there is ~ 10 Å space in between the surfaces of the clusters in the neighboring cells. The Brillouin zone is represented by the Γ point. Several structural possibilities, which include planar and polyhedral forms (see below), have been considered for small sizes with n up to ~ 10 . For larger clusters, growth behaviors based on layered triangular, pyramidal, simple cubic, decahedral (D), I , O , C , and tetrahedral structures have been explored. Initial studies have been done by using USP. The resultant low lying isomers have been re-optimized by using PAW potentials and several new structures for different sizes have been further explored. The energy ordering of isomers changed in some cases for small clusters when PAW method is used. All of the structures are fully optimized without any symmetry constraint by using conjugate gradient method. The convergence criterion for force on each ion is taken to be less than 0.005 eV/Å. For clusters with $n < 40$, spin isomers have also been explored. For large clusters, magnetic moments become generally quite small and magnetic moments obtained from structural optimization have been reported.

III. RESULTS

A. Pt_n clusters: $n=2-10$

Figure 1 shows the lowest energy structures of small clusters ($n=2-10$) along with some competing isomers obtained from PAW method. This range has also been studied by other workers,^{5,10,16} but in some cases, our lowest energy structures are different. Pt_2 is a triplet with a bond length of 2.33 Å and dissociation energy of 3.66 eV. Pt_3 is an equilateral triangle with triplet state and a bond length of 2.49 Å, while Pt_4 is a bent rhombus with a magnetic moment of $4\mu_B$ and a side length of 2.51 Å. A tetrahedron ($2\mu_B$) is nearly degenerate and it lies only 0.07 eV higher in energy, while a square ($0\mu_B$) lies 0.16 eV higher in energy. For Pt_5 , a side capped square (triplet) is 0.14 , 0.23 , and 0.30 eV lower in energy than a trigonal bipyramid ($4\mu_B$), a side capped rhombus ($4\mu_B$), and a square pyramid ($6\mu_B$), respectively. However, a square pyramid becomes important for larger clusters. Up to $n=9$, nearly planar structures are generally favored. Pt_6 has a triangular structure ($6a$) with zero magnetic moment and it is in agreement with the earlier results.⁸ However, we find that the local magnetic moment on each atom is

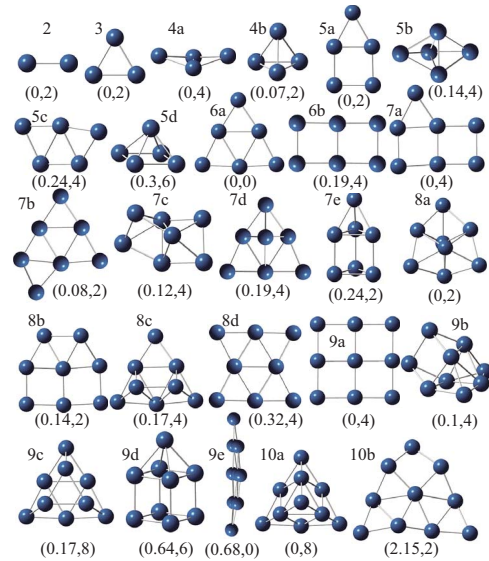


FIG. 1. (Color online) Low lying isomers of Pt_n , where $n = 2-10$. na , nb , etc., are isomers of Pt_n with increasing order of energy. The numbers in brackets refer to the energy (eV) relative to the lowest energy isomer and the magnetic moment (μ_B).

nonzero (see below). This is an important building block of Pt clusters as well as bulk face centered cubic (fcc) structure. A square bicapped on adjacent sides also converges to this isomer, while an isomer with a double square ($6b$) lies 0.22 eV ($4\mu_B$) higher in energy. An octahedron and a prism that are often found to be the ground state for clusters of many elements lie much higher in energy (0.81 and 0.69 eV, respectively) than ($6a$). Pt_7 is a side capped double square ($7a$) with a magnetic moment of $4\mu_B$ and a ferromagnetic coupling. The magnetic moment on different atoms ranges between 0.50 and 0.64 μ_B /atom. This isomer is 0.08 eV ($2\mu_B$), 0.12 eV ($4\mu_B$), 0.19 eV ($4\mu_B$), and 0.24 eV ($2\mu_B$) lower in energy, respectively, than a side capped triangular Pt_6 ($7b$), a bicapped square pyramid that converges to a structure that can be considered to be made of two fused square pyramids ($7c$), a face capped triangular Pt_6 ($7d$), and a prism capped on a triangular face ($7e$). The face capped triangular structure ($7d$) bends, while isomers ($7a$) and ($7b$) also become nonplanar. A face capped octahedron lies 0.41 eV higher in energy than ($7a$) and therefore O isomer is not favored. However, for Pt_8 , an octahedron bicapped on two faces with twofold rotational symmetry converges to a hexagonal bipyramid isomer ($8a$) with a magnetic moment of $2\mu_B$. There are large variations in the local magnetic moment on different sites ranging from -0.01 to 0.51 μ_B /atom with mainly ferromagnetic coupling. A double square bicapped on the long edge (triplet) also becomes nonplanar ($8b$) and lies 0.14 eV higher in energy. A Pt_6 bicapped on face ($8c$) and on sides ($8d$), and a cube, respectively, lie 0.17 eV ($4\mu_B$) and 0.32 eV ($4\mu_B$), and 0.63 eV ($8\mu_B$) higher in energy than ($8a$). Therefore, cubic isomers are not favored in this range.

Pt_9 is planar ($9a$) with four (nearly) squares and a magnetic moment of $4\mu_B$. There is ferromagnetic coupling between the spins with the central atom having the lowest value of $0.21\mu_B$. The atoms on the center of the edges have about 0.42 μ_B /atom magnetic moment, while the corner

sites have $0.53 \mu_B/\text{atom}$ magnetic moment. In this case, a higher coordination tends to reduce the magnetic moment. In general, a lower coordination is expected to lead to a higher magnetic moment, but it is likely that in this case, a stronger bonding between the center and the four neighboring atoms, whose bond length is shorter (2.45 \AA) compared to the nearest neighbors bonds (2.46 \AA) on the sides, also contributes to the reduction in the magnetic moment. A shorter bond length with a higher coordination is contrary to the normal behavior of a shorter bond length for a lower coordination of atoms. A similar behavior was obtained¹⁷ for Rh clusters. The nonmagnetic solution of this isomer lies only 0.06 eV higher in energy, and therefore, the magnetic energy is quite small. Another isomer ($9b$), which can be considered to be formed of fused square pyramids or distorted prism-tetrahedron, lies only 0.1 eV higher in energy and has a magnetic moment of $4\mu_B$. Also, an O isomer with a nearly threefold symmetric tricapping of an octahedron ($9c$) lies only 0.17 eV higher in energy with a high magnetic moment of $8\mu_B$. It can be obtained by adding a layer of three atoms on ($6a$). There is a ferromagnetic coupling between the spins with the capping atoms on octahedron having a lower magnetic moment of about $0.67 \pm 0.05 \mu_B/\text{atom}$, while the atoms in the octahedron have about $1 \pm 0.07 \mu_B/\text{atom}$. This result is also surprising as, in general, a lower coordination atom is expected to have higher spin since Pt atom has a magnetic moment of $2\mu_B$. These results suggest different natures of bonding in planar and three-dimensional (3D) isomers, both of which compete in this size range. The highest occupied molecular orbital–lowest unoccupied molecular orbital (HOMO-LUMO) gap of ($9c$) is 0.17 eV . However, in the energy spectrum of up-spin electrons, the HOMO-LUMO gap is 1.46 eV . A cubic isomer with face capping lies 0.64 eV ($6\mu_B$) higher in energy than ($9a$). Therefore, cubic isomers are unlikely to exist in this size range. Our results for $n=6, 7, 8,$ and 9 clusters differ from those in Ref. 5. The planar-type growth ends here, and beyond $n=9$, 3D structures become more favorable. Indeed, for Pt_{10} , a tetracapped symmetric octahedron ($10a$) derived from ($9b$) by adding an atom in the third layer is highly stable with a magnetic moment of $8\mu_B$ and a tetrahedral morphology. Our result supports the earlier studies on Pt_{10} , but the value of the magnetic moment was reported⁵ to be $6\mu_B$. This isomer lies significantly lower in energy than any other isomer and has high symmetry (tetrahedral) with fcc packing. Note that a distorted triangular structure ($10b$, $2\mu_B$) and a face capped planar isomer of ($9a$) with a magnetic moment of $4\mu_B$ lie 2.15 and 1.22 eV higher in energy, respectively. Also, a cube bicapped on neighboring faces lies 1.15 eV higher in energy than ($10a$). The HOMO-LUMO gap of ($10a$) is 0.24 eV . Similar to ($9c$), the up-spin channel has a large HOMO-LUMO gap of 1.29 eV . The spins are ferromagnetically coupled. The four capping atoms on an octahedron have lower spin magnetic moment of $0.62 \mu_B/\text{atom}$, while the six atoms of the octahedron have $0.92 \mu_B/\text{atom}$. In all of these clusters, triangular and square faces are prominent.

B. Pt_n clusters: $n=11-20$

The low lying isomers of Pt_n , where $n=11-15$, are shown in Fig. 2. Pt_{11} is obtained by adding an atom on a threefold

symmetric site of a face of ($10a$). There are significant distortions in this O structure ($11a$) with nearest neighbor bond lengths varying from 2.55 to 2.99 \AA . The total magnetic moment on this isomer is $4\mu_B$ and the local moment on different sites has a value ranging from -0.03 to $0.74 \mu_B/\text{atom}$ with mainly ferromagnetic coupling. A cubic isomer ($11b$) with threefold symmetric capping on adjacent faces lies 0.21 eV higher in energy with a magnetic moment of $2\mu_B$. Further addition of atoms on ($10a$) can be on the same face or on different faces. For Pt_{12} , a Pt_{10} bicapped on the same face ($12b$, $4\mu_B$) lies 0.03 eV lower in energy than a Pt_{10} bicapped on two faces ($12c$, $4\mu_B$). Also, isomer ($12b$) is 0.12 eV lower in energy than a cube tetracapped on adjacent faces. The latter transforms to a distorted structure shown in ($12d$) having a magnetic moment of $4\mu_B$. However, we find that a triangular bilayer ($12a$) has the lowest energy for Pt_{12} with a magnetic moment of $2\mu_B$. It lies 0.35 eV lower in energy than isomer ($12b$). Therefore, Pt_6 based structures continue to play an important role. We also tried a threefold symmetric trilayer (3,6,3) with a truncated trigonal bipyramid hexagonal closed packed (hcp) structure, but it lies 0.86 eV ($6\mu_B$) higher in energy than ($12a$). Also, an isomer obtained by capping of ($9a$) with three atoms, as shown in ($12e$), lies 0.67 eV higher in energy. Furthermore, an empty center icosahedron for Pt_{12} is highly unfavorable, although it is locally stable and lies 2.27 eV higher in energy than ($12a$). Pt_{13} is obtained from ($12a$) by capping an atom on a threefold site, as shown in ($13a$) in Fig. 2(a). It has a magnetic moment of $2\mu_B$. A similar result was obtained by Wang and Johnson.³ Also, an isomer with a tetrahedron capped on ($9a$), as shown in ($13b$), is nearly degenerate and it lies only 0.01 eV higher in energy with a magnetic moment of $2\mu_B$. An O isomer obtained from ($12c$) by further adding an atom on a face, as shown in ($13c$), symmetrically lies 0.21 eV higher in energy with a magnetic moment of $4\mu_B$. Also, if an atom is added on a face of ($12b$), then isomer ($13d$) is obtained that lies 0.32 eV higher in energy than ($13a$) with a magnetic moment of $4\mu_B$. A cubic isomer ($13e$) with five faces capped lies 0.38 eV higher in energy. In this case, all of the atoms have zero magnetic moment. An isomer in which four atoms cap isomer ($9a$), as shown in ($13f$), lies 0.39 eV higher in energy than ($13a$). The four atoms do not symmetrically cap the four squares. However, for Pt_{14} , a nonmagnetic square pyramid based on ($9a$) has the lowest energy. It ($14a$) combines the two best small size clusters, namely, $n=6$ and 9 with four ($6a$)- and one ($9a$)-type faces and no atom inside the pyramid. An O isomer with all of the eight faces of an octahedron capped ($14b$, $4\mu_B$) lies 0.2 eV higher in energy than ($14a$). It is the cube of fcc structure but with two significantly different bond lengths of $\sim 2.55 \text{ \AA}$ (connected in Fig. 2) and 2.95 \AA within the octahedron. However, a cubic isomer of Pt_{14} with all of the faces of a cube covered lies 1.08 eV ($2\mu_B$) higher in energy than ($14a$). A threefold symmetric O isomer ($14c$, $0\mu_B$) obtained from ($13d$) with a trigonal bipyramid structure lies 0.24 eV higher in energy than ($14a$). Both ($14b$) and ($14c$) O isomers are nearly degenerate and have atomic shell closing. Also, isomer ($14a$) has atomic shell closing. We also tried an isomer by adding an atom on ($13a$), as shown in ($14d$), but it lies 0.37 eV higher in energy. In this case, the symmetry of the structure is broken, but for

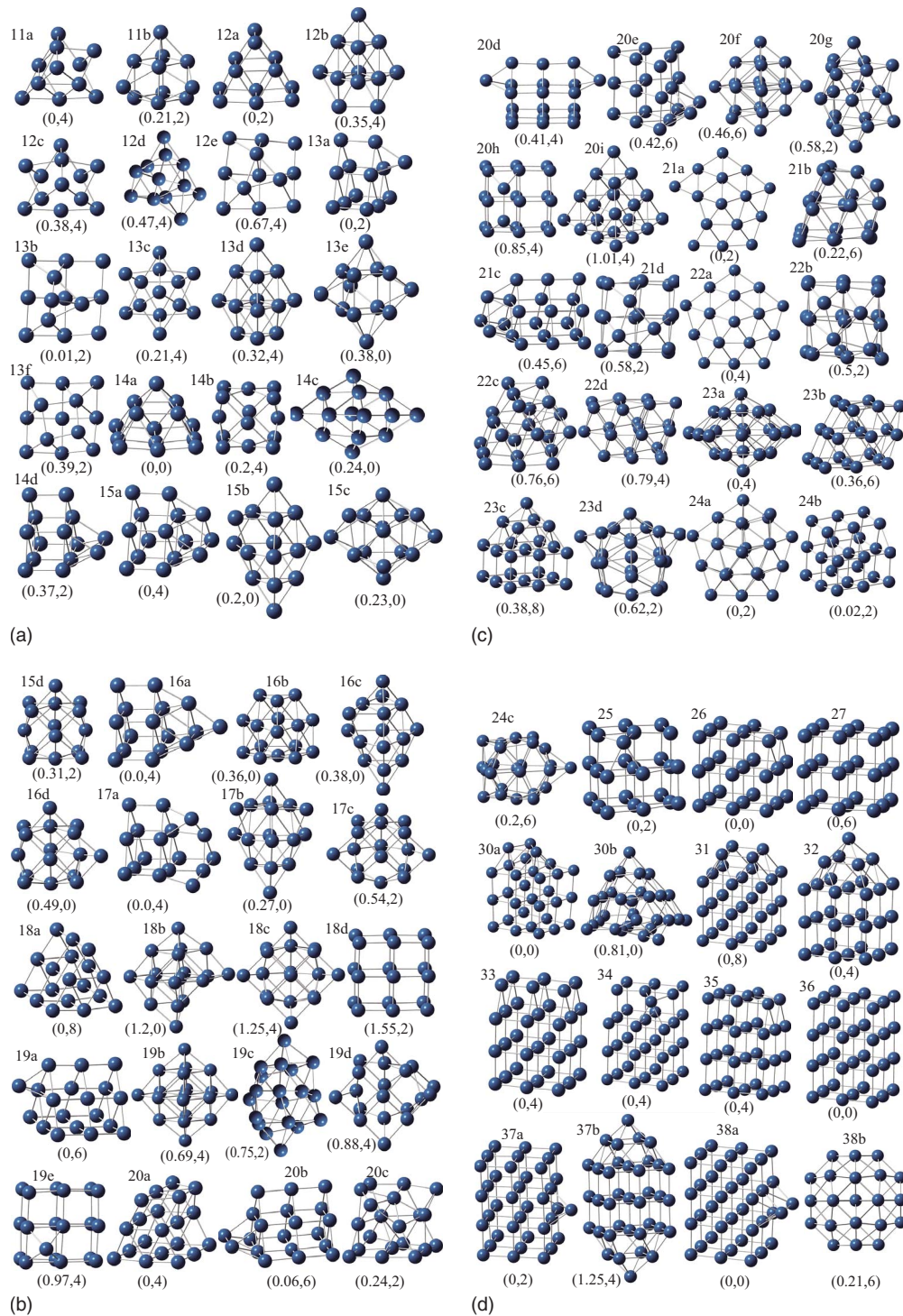


FIG. 2. (Color online) (a) Low lying isomers of Pt_n clusters, $n=11-15$. (b) Continued from Fig. 2(a) and low lying isomers for $n=16-20$. (c) Continued from Fig. 2(b) and for $n=21-24$. (d) Continuation of Fig. 2(c) and for $n=25-38$ except for $n=28$ and 29.

Pt_{15} , addition of an atom on (14d) leads to the lowest energy structure as shown in (15a). Therefore, symmetric structures play an important role. An isomer (15b) obtained from capping of a threefold symmetric site of (14c) lies 0.2 eV higher in energy. All of the atoms in this isomer have zero magnetic moment. Another isomer (15c) obtained from an empty center Frank–Kasper polyhedron lies 0.23 eV higher in energy with zero magnetic moment. It transforms to a capped cubic

structure. Also, an isomer obtained from (14b) by capping an atom on an edge [15d in Fig. 2(b)] lies 0.31 eV ($2\mu_B$) higher in energy. Therefore, triangular layered, cubic, and O isomers lie close in energy in this size range.

Pt_{16} is obtained from (15a) by adding an atom such that a tetrahedral (10a) cluster caps (6a), as shown in (16a) in Fig. 2(b). It has a magnetic moment of $4\mu_B$. An empty center 16-atom Frank–Kasper (FK) polyhedron converges to a lay-

ered fcc structure with a tetrahedral symmetry (16*b*) and a zero magnetic moment on all of the atoms. It lies 0.36 eV higher in energy than (16*a*). An isomer (16*c*) obtained from (14*c*) by capping two faces lies 0.38 eV ($0\mu_B$) higher in energy. In this case, the zero magnetic moment arises due to an antiferromagnetic coupling between the spins, but the magnetic moment on each atom is small ranging from $-0.07\mu_B$ to $0.12\mu_B$. Another isomer (16*d*) obtained from (14*b*) by capping two adjacent sides lies 0.49 eV higher in energy. It has a magnetic moment of $2\mu_B$ with ferromagnetic coupling. The lowest energy structure of Pt₁₇ is obtained from Pt₁₈ (18*a*) by removing an atom. (18*a*) is obtained from the stacking of three layers of (6*a*) triangular isomer. This prism structure is again a combination of the lowest energy isomers (6*a*) and (9*a*) and it is exceptionally stable with significantly lower energy than any other isomer and relatively high magnetic moment ($8\mu_B$). Another isomer of Pt₁₇ is obtained from (14*c*) by threefold symmetric capping of faces by three atoms (17*b*) or adding an atom on (16*c*). It has packing of triangular layers and it lies 0.27 eV higher in energy than (17*a*). The net magnetic moment is zero, but the magnetic moment on atoms varies from -0.14 to $0.16 \mu_B/\text{atom}$, and therefore, the coupling between the spins is also antiferromagnetic. A 17-atom FK polyhedron with a central atom lies 1.78 eV higher in energy suggesting that high coordination continues to be unfavorable. Isomers with an atom capped on a threefold symmetric site of (16*b*) and tricapping of (14*b*) (as shown in 17*c*) lie 0.71 eV ($2\mu_B$) and 0.54 eV ($2\mu_B$) higher in energy, respectively. We also considered the 3×4 and 4×4 square meshes for $n=12$ and 16, but these get distorted and lie 1.54 and 3.42 eV higher in energy than 3D structures (12*a*) and (16*a*), respectively. Also a $2\times 1\times 1$ cubic column for $n=12$ lies 1.04 eV higher in energy than (12*a*). These results suggest preference for relatively open structures with 3D triangular and triangular-square networks in this size range.

For Pt₁₈, we also tried a few other isomers but all lie much higher in energy compared to (18*a*). A centered octahedron with an atom removed from an edge (18*b*, $0\mu_B$) lies 1.2 eV higher in energy. The magnetic moment on each atom in this isomer is small ($\sim 0.02\mu_B$) with an antiferromagnetic coupling. *O* isomers, in which an atom is removed from a corner or the central site, lie still higher in energy. A $2\times 2\times 1$ cubic isomer (18*d*) with two layers of Pt₉ (9*a*) cluster lies 1.55 eV ($2\mu_B$) higher in energy and an *O* isomer (18*c*) obtained from capping of (17*c*) (no center atom) lies 1.25 eV ($4\mu_B$) higher in energy. Therefore, the *O* growth with and without a center atom competes with each other, but these are not favorable. For Pt₁₉, an isomer with one atom capping isomer (18*a*), as shown in (19*a*) in Fig. 2(*b*), is the lowest in energy with a magnetic moment of $6\mu_B$. Another isomer, in which an atom caps a triangular face on the central triangle, lies only 0.08 eV higher in energy. Also, an isomer, in which an atom caps a square on a square face, lies 0.13 eV higher in energy than (19*a*). Therefore, adding an atom on (18*a*) at different threefold or fourfold sites changes the energy only a little. We also tried a few other isomers. A centered octahedron (19*b*, $4\mu_B$), which is an isomer obtained by capping five atoms on (14*c*), capping five atoms on (14*b*), as shown in (19*d*) with $4\mu_B$, and a capped cubic structure (19*e*, $4\mu_B$), respectively, lie

0.69, 0.75, 0.88, and 0.97 eV higher in energy than (19*a*). Therefore, the growth by capping the layered triangular structure of (18*a*) is highly favorable. Accordingly, the lowest energy structure of Pt₂₀ is obtained from (18*a*) by capping two atoms on a square face, as shown in (20*a*). It has a magnetic moment of $4\mu_B$. Another isomer (20*b*), in which two atoms cap a triangular face of (18*a*), is nearly degenerate with only 0.06 eV higher energy and a magnetic moment of $6\mu_B$. An isomer [20*d* in Fig. 2(*c*)], in which one atom is capped on each of the two triangular faces of (18*a*), lies 0.41 eV higher in energy than (20*a*). Therefore, capping atoms tend to be nearest neighbors. An isomer obtained from (14*b*) by capping six atoms on edges transforms to a distorted structure shown in (20*c*). It has (9*a*) as a part, on which 11-atom subcluster is attached. It shows the importance of (9*a*) in building larger clusters (see also below). Another isomer obtained by a different capping of two atoms on (18*a*) on a square face, as shown in (20*e*) in Fig. 2(*c*), lies 0.42 eV higher in energy. Therefore, there is a strong preference in the way atoms are added on (18*a*). An isomer obtained from (19*b*) by a threefold symmetric capping on a face (20*f*, $6\mu_B$) lies 0.46 eV higher in energy than (20*a*), while an isomer (20*g*) with six atoms added on (14*c*) lies 0.58 eV ($2\mu_B$) higher in energy. A tetrahedral isomer (20*i*), which is most favorable for Au,¹⁸ an element next to Pt, and a bicapped cubic isomer (20*h*), lie 1.01 eV ($4\mu_B$) and 0.85 eV ($4\mu_B$) higher in energy, respectively. Therefore, in the size range of 11–20 atoms, layered triangular structures are generally favored, and in some cases, *O* isomers as well as cubic isomers compete. Clusters of many elements favor *I* growth among the close packed structures. However, for Pt, we find that *I* isomers lie significantly higher in energy in all of the cases.

C. Pt_n clusters: $n=21-24$

In the range of $n=21-24$, *D* isomers become most preferred. For Pt₂₂, an empty center *D* cage (22*a*), as shown in Fig. 2(*c*), has the lowest energy with a fivefold rotational symmetry and a magnetic moment of $4\mu_B$. In this isomer, one can see ten triangular faces of (6*a*) type that are fused together. This result shows the continuous importance of triangular faces with (6*a*) units and the relatively open structures that Pt clusters continue to favor. Pt₂₁ is obtained from Pt₂₂ by removing an atom from an edge, while Pt₂₃ is obtained by adding an atom inside the decahedron of Pt₂₂. Removing an atom from a vertex to keep fivefold rotational symmetry is not favored, as it disturbs the triangular structures in five faces, while removing an atom on an edge, as shown in (21*a*) in Fig. 2(*c*), disturbs only two triangular faces. We also considered isomers with three atoms capping on (18*a*) on a square face (21*b*) and on a triangular face (21*c*). These isomers lie 0.22 and 0.45 eV higher in energy, respectively, with a magnetic moment of $6\mu_B$ on each. Also, we considered three atoms capping on a Pt₁₈ cubic isomer, as shown in (21*d*), and it also lies 0.58 eV higher in energy than (21*a*). Similar to Pt₂₁, we also tried capping of four atoms on a square face of (18*d*) and (18*a*), as shown in (22*b*) and (22*c*) to obtain isomers of Pt₂₂, but both of these lie signifi-

cantly higher in energy than (22a). Also, an isomer obtained from three atoms capping a *C* isomer (19b) converges to (22d) and it lies 0.79 eV higher in energy than (22a). These results also suggest that the *D* isomer of Pt₂₂ is significantly more stable than other isomers, and therefore, this cage structure has a special stability.

In the case of Pt₂₃, we considered a *D* isomer with an atom inside Pt₂₂ cage. Upon optimization, the atom inside the Pt₂₂ *D* cage is slightly displaced from the center. We also tried capping of a square pyramidal Pt₅ unit on a square face of (18a) and (18d). Both the converged structures are nearly degenerate and lie 0.36 and 0.38 eV higher in energy than (23a), as shown in (23b) and (23c), respectively, with $6\mu_B$ and $8\mu_B$ magnetic moment. A polyicosahedral isomer of Pt₂₃ (three interconnected 13-atom icosahedra) converges to a structure shown in (23d) and it lies 0.62 eV higher in energy than (23a), suggesting again that *I* isomers are quite unfavorable. For Pt₂₄ isomers with *D*, layered triangular as well as cubic structures become nearly degenerate and it suggests a possible transition to another growth mode. Note that the energy difference of cubic isomers with respect to the lowest energy isomers is continuously decreasing as the cluster size grows from $n=18$ to 24 and in the case of Pt₂₄, a cubic isomer (24b) with six atoms capped on a square face of (18d) is nearly degenerate with a *D* isomer (24a), in which an atom caps on a triangular face of Pt₂₃. These results point to the increasing importance of cubic isomers beyond $n=24$. For Pt₂₄, we also tried four layers of (6a), but this isomer lies 0.81 eV higher in energy than (24a). Therefore, layered growth of (6a) triangular units is favored only up to three layers and with partial covering in the fourth layer. An *I* isomer obtained from capping of *I*-Pt₂₃ converges to a structure shown in (24c) in Fig. 2(d) and it is only 0.2 eV higher in energy than (24a). In this isomer, approximately three layers with triangular nets can be seen.

D. Pt_{*n*} clusters: $n=25-44$

Beyond $n=24$, cubic isomers have the lowest energy with high stability of Pt₂₇ that has $3 \times 3 \times 3$ cubic units. In Fig. 2(d), we have shown the cubic growth ranging from $n=25$ to 38 by successive addition of atoms except for $n=28$ and 29 for which convergence was not obtained. We also tried a few other isomers in this size range, but our search is not exhaustive. For Pt₂₇, we tried an isomer derived from Pt₁₈ trigonal prism by adding a base of Pt₉ on one of the square faces. This converges to the cubic isomer, suggesting the preference for cubic isomer. In the case of $n=30$, we optimized a pyramidal isomer by adding a 4×4 square base on Pt₁₄ pyramid. The optimized structure [30b in Fig. 2(d)] shows distortions and it lies 0.81 eV higher in energy than a cubic isomer (30a), in which three atoms cap on a square face of (27a). Therefore, continuation of pyramidal growth is not favored. Pt₃₁ is obtained from Pt₃₀ by the addition of one more atom on the square face, while for Pt₃₂, we find further addition of an atom on top of the four atoms to be favorable. This isomer can be considered to be formed of a (14a) pyramid on cubic isomer (18d). Further additions of atoms lead to cubic isomers of Pt₃₃, Pt₃₄, and Pt₃₅, as shown in Fig. 2(d). Our results

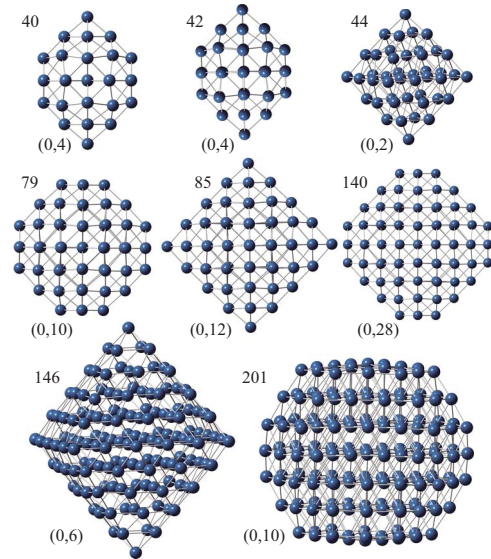


FIG. 3. (Color online) Same as in Fig. 2 but for octahedral clusters with n value given in each case.

suggest that a cubic isomer of Pt₃₆ with four layers of Pt₉ is particularly stable and the layered growth based on (9a) saturates around this size. For larger clusters, we optimized cubic isomers by capping two atoms on Pt₃₆ either on a 3×3 face or on a 3×4 face. We find a symmetric capping of Pt₃₆ on a 3×4 face, as shown in (38a), to be slightly more favorable than the capping on a 3×3 face. Similarly, for $n=37$, an isomer, in which an atom caps on a 3×4 face (37a), is 1.25 eV lower in energy than an isomer, in which pyramids of 14-atoms are made on opposite faces with a Pt₉ inserted in between, as shown in (37b). Even though parts of this isomer form magic clusters, their assembly is not of the lowest energy. The cubic isomer of Pt₃₈ is nearly degenerate with a truncated *O* isomer, as shown in (38b). Therefore, beyond $n=38$, we considered capping of the isomer (38b). Interestingly, for Pt₄₀ as well as Pt₄₂, we find that cubic isomers with four and six atoms capped on Pt₃₆ have higher energy than the *O* isomers (Fig. 3), in which two and four atoms are capped on opposite square faces. The reason for the lowering of the energy of the *O* isomers by addition of atoms on vertices is that it leads to the formation of (6a) triangular units, which are energetically highly preferred. Capping by one atom leads to the formation of four such (6a) units and in the case of Pt₄₄, we obtain an *O* isomer (Fig. 3), in which all the six vertices are capped. This is also a very stable isomer in this size range. It has two octahedral layers: an inner octahedron of Pt₆ and an outer shell of Pt₃₈. We removed the inner octahedron to check if a cage structure with triangular faces would be favored, but the converged structure lies 3.74 eV higher in energy than (38a). Similarly, we also tried an *I* cage of Pt₄₂ derived from *I*-Pt₅₅ by removing the inner icosahedron of 13 atoms. This isomer has all triangular faces. However, it lies 3.67 eV higher in energy than the lowest energy *O* isomer. Therefore, the empty cages are not favored in this size range.

E. Large clusters—octahedral growth

In order to further explore the possibility of a transition to a close packed *I* growth, we studied 55-, 147-, and 309-atom

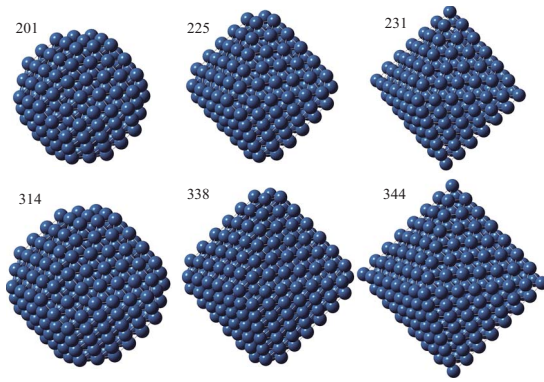


FIG. 4. (Color online) Optimized atomic structures of large octahedral and truncated octahedral clusters. Clusters with $n=231$ and 344 have fully triangular faces. In the case of $n=225$ and 338, six atoms have been removed from vertices, while in the cases of $n=201$ and 314, five atoms have been removed from each vertex.

I ($10\mu_B$, $26\mu_B$, and $0\mu_B$, respectively), D ($10\mu_B$, $2\mu_B$, and $4\mu_B$, respectively), and C ($10\mu_B$, $2\mu_B$, and $0\mu_B$, respectively) isomers by using USP. While I isomers are 1.00, 0.55, and 1.08 eV and 1.06, 1.17, and 1.58 eV lower in energy than D and C isomers, respectively, we find that the O clusters have the lowest energy even in the range of such large clusters. Calculations with PAW potentials gave the same trend. We studied the O clusters without a central atom ($n=44$ as above, 146, and 344; truncated octahedra with $n=38$ as above, 116, 140, 314, and 338) as well as the O clusters with a central atom ($n=79$, 85, 225, and 231). We also considered cubic columnar structures $3 \times 3 \times p$ for $n=45$ ($p=5$) and 54 ($p=6$), but these are not among the lowest energy isomers in this size range. Also, we considered a $4 \times 4 \times 4$ cubic isomer of Pt_{64} . The converged cubic structure is stable and it shows that such open structures are possible from a bonding point of view. However, their binding energy (BE) per atom (BE is defined with reference to free atoms) is not much favorable as it is lower than the value for O - Pt_{44} . Therefore, the cubic growth is unlikely in this size range. For larger clusters, the optimized O structures are shown in Figs. 3 and 4. In general, there are small relaxations from idealized structures. Our results show that O - Pt_{146} ($6\mu_B$) is 2.23 eV lower in energy than I - Pt_{147} . Also, I - Pt_{146} with an atom removed from either center or vertex lies significantly higher in energy. Similarly, O - Pt_{314} has 0.056 eV/atom higher BE than I - Pt_{309} , which is a very significant energy difference in this size range by addition of only five atoms. Further, as a test case, we heated the O isomer of Pt_{231} up to 600 K and cooled it to 0 K at an interval of 200 K for about 1.3 ps. However, no structural change has been obtained. From the above results, we conclude that clusters and/or nanoparticles with at least up to around 350 atoms (~ 3 nm diameter) favor the O growth beyond $n \sim 40$ and that the I growth is quite unfavorable. This is a very unusual result that bulk structure is favored from a relatively small size range of about 40 atoms (also even for some smaller clusters) and is continued for quite large clusters that have been studied here. Clusters of many elements favor the I growth either beginning from a small size range or the I structures become favorable with an increase in size such as for Au. In such cases, finally, a tran-

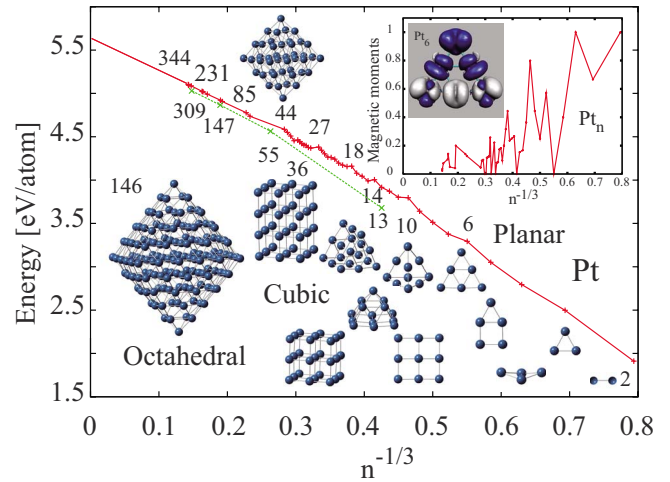


FIG. 5. (Color online) Binding energy as a function of $n^{-1/3}$. The red (with plus points) and green (with crosses) curves correspond to the lowest energy and I isomers, respectively. The numbers of atoms for selected clusters are marked, and in several cases, their structures have also been shown. The growth regimes where planar, cubic, and O structures dominate have been indicated. Beyond $n=344$, the binding energy curve has been linearly extrapolated to the bulk limit. The inset shows the magnetic moment per atom as a function of $n^{-1/3}$. It shows an oscillatory behavior with decreasing trend with increasing size. The magnetic moment becomes quite small for $n \sim 231$. However, clusters with truncated O structures have significantly higher magnetic moment. An isosurface of spin polarization for Pt_6 is also shown. It has ferromagnetic-antiferromagnetic coupling. The blue (dark color) and white (light color) surfaces correspond to up and down spin density distributions, respectively.

sition should occur to bulk structure with an increase in n . However, for Pt clusters, it remains to be seen if a transition would ever occur to I structures.

F. Binding energy

Figure 5 shows the BE as a function of $n^{-1/3}$. In general, the BE of the lowest energy isomers is significantly higher compared to the I isomers. With increasing size, the BE of the I isomers becomes closer to the value for the O isomers, but a crossover does not seem imminent. In the small size range, a local maximum in the BE can be seen for $n=6$, 10, 14, 18, 22, and 27 and these are the magic clusters with atomically closed shells and symmetric structures, such as a triangle, tetrahedron, square pyramid, layered triangular prism, empty center decahedron, and a cube, respectively. Pt_{10} is also experimentally known to be a magic cluster.¹⁹ However, the HOMO-LUMO gap is not large (within about 0.27 eV). Pt_{27} and Pt_{36} with $3 \times 3 \times 3$ cube and $3 \times 3 \times 4$ cubic columns, respectively, have locally high BEs and are likely to be abundant. For Pt_{36} , the BE per atom is higher than the value for truncated O Pt_{38} , but larger columns, such as $3 \times 3 \times 5$ and $3 \times 3 \times 6$ with $n=45$ and 54, respectively, have lower BEs compared to other clusters in this range. Our results suggest that the O clusters *without* truncation are generally more favored, as discussed above due to the formation

of triangular faces. One can notice a significant rise in the BE going from 38 to 44 and from 79 to 85. In the limit $n \rightarrow \infty$, the BE approaches the calculated bulk cohesive energy of 5.57 eV/atom, which is a slight underestimation from the experimental value of 5.84 eV/atom. An improvement in agreement with the experiment can be expected if full relativistic effects are taken in to account.

G. Electronic structure and magnetism

Our results show that Pt clusters are weakly magnetic, which is in agreement with experiments. The magnetic moment decreases as the size increases with an oscillatory behavior (inset in Fig. 5). For Pt₁₃, the calculated value is 0.15 μ_B /atom (two unpaired electrons) compared to eight unpaired electrons reported¹ for clusters in zeolite cages, whose size was estimated to be 13 ± 2 atoms by assuming *I* structure. Thirteen-atom cluster is unlikely as *I*-Pt₁₃ is very unfavorable and the magnetic moment of the lowest energy isomer is much lower than inferred from experiments. The spin isomer of Pt₁₃ with a magnetic moment of $4\mu_B$ lies 0.16 eV higher in energy and spin isomers of still higher magnetic moment would be even more unfavorable. Also, other low lying isomers of Pt₁₃ have low magnetic moments. Therefore, an interesting question is whether magnetic moment is enhanced when clusters are in zeolite cages. The other possibility is that the clusters could have ten atoms, which is a magic cluster size and it has a magnetic moment of $8\mu_B$. Clusters with $n=6, 14,$ and 36 have zero magnetic moment. In the case of $n=6$, the local moments are nonzero due to antiferromagnetic coupling (see inset in Fig. 5). For $n=14$ and 36 , the local moments are quite small and the net magnetic moment is zero due to antiferromagnetic coupling. An interesting question is the change in the distribution of the magnetic moments of the Pt₆ triangular layer when two and three such layers are present as in Pt₁₂ and Pt₁₈. In the case of Pt₁₂, the outer six atoms on the vertices of the triangles have small magnetic moments ($-0.01\mu_B$), while the prism formed by the centers of the edges are ferromagnetically coupled each with a magnetic moment of $0.35\mu_B$. After adding one more layer, the whole cluster becomes ferromagnetic. By considering the whole cluster as a prism, the six vertices of this prism have a magnetic moment of $0.35\mu_B$ /atom, while the centers of the three edges (connecting the two triangles of the prism) have a magnetic moment of $0.26\mu_B$. The centers of the square faces have $0.49\mu_B$ /atom, while the remaining six edge centers lying on the outer two triangular faces have a magnetic moment of $0.61\mu_B$. Therefore, the lowest coordinated site does not have the highest magnetic moment. Also, it is interesting to see the change in the distribution of the magnetic moments going from Pt₉ to Pt₂₇. We find that both Pt₉ and Pt₂₇ are ferromagnetic. For Pt₂₇, the center of the cube has nearly zero magnetic moment, while the corners of the cube, centers of the faces, and the centers of the edges have magnetic moments of $0.20\mu_B, 0.22\mu_B,$ and $0.26\mu_B$, respectively. Therefore, in this case, the magnetic moment is nearly uniform except for the center of the cluster, and in general, there is a decrease in the magnetic moment. For large clusters, the magnetic moment is generally small.

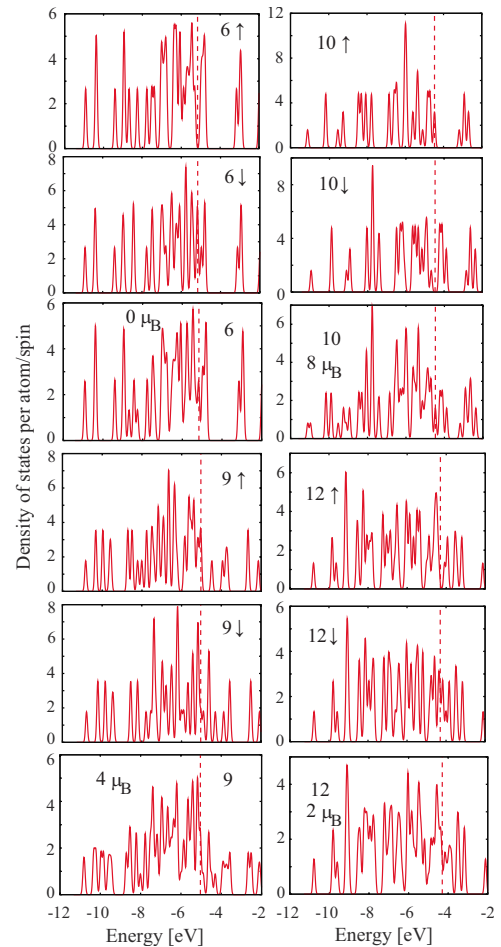


FIG. 6. (Color online) Gaussian broadened (half width of 0.05 eV) electronic states of clusters with $n=6, 9, 10,$ and 12 . Both the spin-polarized and total densities of states have been shown. The magnetic moments in the lowest energy isomer are also given. The vertical dashed line shows the HOMO.

The electronic states of a few selected clusters are shown in Figs. 6 and 7. As most of the clusters are magnetic, we have shown the spin polarized as well as the total density of states obtained from Gaussian broadening (half width of 0.05 eV) of the energy levels. There appears no systematic pattern as the structures are different. With an increase in the size of the clusters, the distribution of the states becomes dense as expected, and at around $n=20$, the spectrum becomes nearly continuous. The electronic states of the simple cubic clusters (Fig. 8) with $n=27$ and 36 are similar. The spectra have sharp peaks due to the relatively open structures of these clusters. These significantly differ from the spectra for the decahedral clusters, as it can be seen for $n=22$ in Fig. 7. In the case of the magic clusters with $n=6, 9, 14, 18, 22, 27,$ and 36 , the HOMO lies in a region of low density of states, indicating that there is more significant HOMO-LUMO gap for these clusters compared to other cases.

The Gaussian smeared electronic states of the selected *O* clusters are shown in Fig. 9. These results show that even for $n=44$ and 85 , there are significant quantum size effects and the spectra have many spikes. For larger clusters with $n=146, 231,$ and 344 , the features of the bulk spectrum start

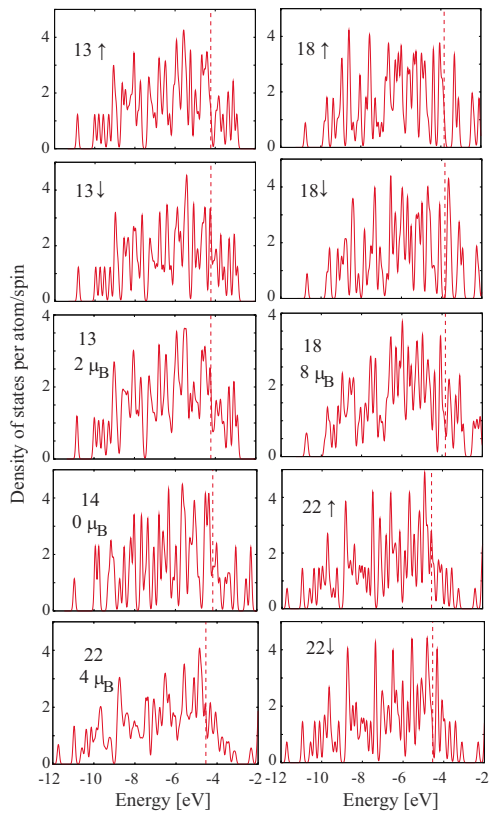


FIG. 7. (Color online) Same as in Fig. 6 but for $n=13, 14, 18,$ and 22 . For $n=14$, the cluster is nonmagnetic, and therefore, only the total density of states has been shown.

arising as one can see from the density of states away from the HOMO. However, close to the HOMO, the difference from the density of states of bulk Pt(111) surface is significant and it is due to a large fraction of atoms on the surface in clusters. All of the faces in these O clusters are (111) type, but there is a significant fraction of low coordination sites due to edges and vertices, which can be expected to significantly contribute to the electronic states in the vicinity of the HOMO level and this can make a difference to the reactivity of clusters compared to bulk (111) surface.

IV. SUMMARY AND DISCUSSION

In summary, we have studied the atomic growth behavior of Pt_n clusters in a wide range of sizes starting from two

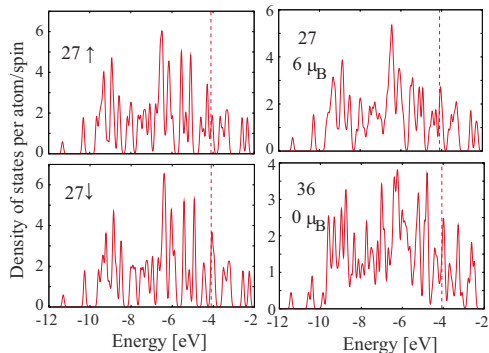


FIG. 8. (Color online) Same as in Fig. 6 but for simple cubic clusters with $n=27$ and 36 .

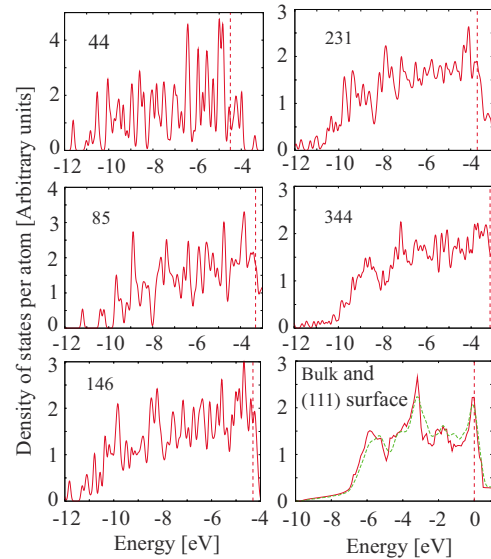


FIG. 9. (Color online) Gaussian broadened total electronic spectra per spin of octahedral Pt_n clusters. The value of n is given in each case. The vertical line shows the HOMO. The densities of states for bulk (full curve) and (111) surface (broken line) are also shown with the Fermi energy taken as the zero of energy.

atoms to nanoparticles having a diameter of about 3 nm. In the small size range with $n < 10$, the clusters generally prefer planar structures and there are two prominent structural units: (i) a triangle of Pt_6 and (ii) a square for Pt_9 that play a very important role in the growth of larger three dimensional clusters. The magic clusters tend to optimize the number of such units. For $n=10$, there is a tetrahedral structure with four triangular units of Pt_6 . It is an octahedron with four faces capped such that it has tetrahedral symmetry. It is exceptionally stable in this size range. Therefore, the octahedral structure is preferred and it competes with other isomers. For Pt_{14} , a square pyramid with a Pt_9 base and four Pt_6 faces is the lowest in energy. Another particularly stable structure is obtained for $n=18$ which has a layered structure formed from three Pt_6 triangles such that it forms a triangular prism with three Pt_9 faces and two Pt_6 faces. Pt_{12} is formed by two Pt_6 layers, but it is not a magic cluster as it has three double square faces. These results suggest that with growing n , the number of square faces increases, and for Pt_{27} , all of the six faces are Pt_9 -type squares. The formation of complete triangles is important. In the range of $20 < n < 25$, decahedral isomers are preferred as the number of Pt_6 triangles is maximized. Beyond $n=27$, our search is not extensive, but our results suggest simple cubic structures to be generally favorable up to $n=38$ with Pt_{36} having $3 \times 3 \times 4$ cubic units to be particularly stable. A truncated octahedral isomer of Pt_{38} is not of lowest energy due to the absence of the complete triangular faces. Completion of the triangular faces lead to the lowering of the energy and Pt_{44} becomes a magic cluster. We tried icosahedral isomers but found them to be unfavorable. Therefore, our results suggest that platinum clusters tend to have high dispersion with 10-, 14-, 18-, and 22-atom magic clusters having all the atoms on the surface and 27-atom cluster has only one atom inside. This reduces the electronic kinetic energy. The icosahedral growth, which is often

found in a large variety of clusters, is not favored by Pt clusters. Also, simple cubic structures are unlikely beyond $n \sim 40$. We find octahedral clusters to be more favorable for $n \geq 40$. Therefore, we find bulk structure is favored from a surprisingly small size (about 40 atoms and onwards) and it is continued for clusters with at least $n \sim 350$ that we have studied. This makes Pt clusters unique among the known clusters of elemental transition metals. It remains to be seen if there would be a transition to often found icosahedral growth for larger n , but the chances are low. This is in striking contrast to isoelectronic Ni and Pd clusters that are icosahedral. We find small magnetic moments in Pt clusters, which is in agreement with experiments. As the size increases, the magnetic moments tend to decrease with an oscillatory behavior. There are ferromagnetic and antiferromagnetic couplings between the spins in some cases. The electronic structures of even the large octahedral clusters differ from bulk (111) surface due to large dispersion and the

presence of low coordination sites, such as edges and vertices. The nearly planar as well as other open structures in the small size range should make it possible to design Pt particles with different structures and properties. It would be of interest to explore the reactions on different structures and model novel catalysts by addition of other elements, which could have significant effect on the structure and properties of Pt clusters.

ACKNOWLEDGMENTS

V.K. gratefully acknowledges the kind hospitality at IMR and the International Frontier Center for Advanced Materials and the support of M. W. Chen. We thank the staff of the Center for Computational Materials Science for the use of the supercomputing facilities and P. Murugan and R. Note for computational help.

-
- ¹X. Liu, M. Bauer, H. Bertagnolli, E. Roduner, J. van Slageren, and F. Phillipp, *Phys. Rev. Lett.* **97**, 253401 (2006).
²V. Kumar and Y. Kawazoe, *Phys. Rev. B* **66**, 144413 (2002).
³L.-L. Wang and D. D. Johnson, *Phys. Rev. B* **75**, 235405 (2007).
⁴E. K. Parks, L. Zhu, J. Mo, and S. J. Riley, *J. Chem. Phys.* **100**, 7206 (1994).
⁵L. Xiao and L. Wang, *J. Phys. Chem. A* **108**, 8605 (2004).
⁶E. Apra, F. Baletto, R. Ferrando, and A. Fortunelli, *Phys. Rev. Lett.* **93**, 065502 (2004).
⁷N. Watari and S. Ohnishi, *Phys. Rev. B* **58**, 1665 (1998).
⁸S. H. Yang, D. A. Drabold, J. B. Adams, P. Ordejon, and K. Glassford, *J. Phys.: Condens. Matter* **9**, L39 (1997).
⁹C. M. Chang and M. Y. Chou, *Phys. Rev. Lett.* **93**, 133401 (2004).
¹⁰T. Futschek, J. Hafner, and M. Marsman, *J. Phys.: Condens. Matter* **18**, 9703 (2006).
¹¹G. Kresse and J. Furthmuller, *Phys. Rev. B* **54**, 11169 (1996).
¹²G. Kresse and J. Hafner, *Phys. Rev. B* **47**, 558 (1993).
¹³G. Kresse and D. Joubert, *Phys. Rev. B* **59**, 1758 (1999).
¹⁴P. E. Blöchl, *Phys. Rev. B* **50**, 17953 (1994).
¹⁵J. P. Perdew, in *Electronic Structure of Solids'91*, edited by P. Ziesche and H. Eschrig (Akademie, Berlin, 1991).
¹⁶K. Bhattacharyya and C. Majumder, *Chem. Phys. Lett.* **446**, 374 (2007).
¹⁷Y.-C. Bae, V. Kumar, H. Osanai, and Y. Kawazoe, *Phys. Rev. B* **72**, 125427 (2005).
¹⁸J. Li, X. Li, H.-J. Zhai, and L.-S. Wang, *Science* **299**, 864 (2003).
¹⁹C. Adlhart and E. Uggerud, *Chem. Commun. (Cambridge)* **2006**, 2581.